Available online at www.sciencedirect.com
ScienceDirect
Journal of Catalysis 244 (2006) 10–16
JOURNAL OF CATALYSIS
www.elsevier.com/locate/jcat

A systematic theoretical study of water dissociation on clean and oxygen-preadsorbed transition metals

Gui-Chang Wang *, Shu-Xia Tao, Xian-He Bu *

Department of Chemistry, Nankai University, Tianjin 300071, PR China

Received 1 April 2006; revised 4 July 2006; accepted 21 July 2006

Available online 25 September 2006

Abstract

Water dissociation on clean and oxygen-preadsorbed transition metal surfaces was investigated by the DFT-GGA method. The total energy change and the reaction barrier were calculated with respect to the direct and oxygen-assisted cleavage of O–H bonds of water. The calculated results showed periodic trends for water dissociation on both clean and oxygen-preadsorbed surfaces. On clean surfaces, the chemical activity for water dissociation increases in the order of Au < Ag < Cu < Pd < Rh < Ru < Ni; on oxygen-preadsorbed surfaces, the inducing effect decreases in the above order with a strongly facilitating O–H bond cleavage on the inactive metals Au, Ag, and Cu; a moderate inducing effect on Pd and Rh; and little effect on Ru and Ni surfaces. We found an interesting relationship between the adsorption energy of oxygen atom on the given metal surfaces and the difference between the activation barrier of clean metal surfaces and that of oxygen-preadsorbed metal surfaces. That is, the more strongly the oxygen atoms bound to the metal surface, the less promoting effect they have on the water O–H bond scission. Our results are in general agreement with previous experimental observations.

Keywords: Water dissociation; Oxygen-preadsorbed; DFT-GGA; Transition metal surfaces; Slab model; Activation barrier

1. Introduction

The outcome of many catalytic processes can be altered dramatically by introducing a small amount of promoters that speed up certain reaction steps or poisons that can slow particular reaction steps [1]. Controlling a reaction path by modifying the catalysts is of considerable importance in surface science and heterogeneous catalysis; thus, all efforts to clarify the role of modifiers on catalyst surfaces toward relevant routes are worthy [2]. In recent decades, much work has been devoted to the effect of the preadsorbed oxygen on the activity of the transition metal surfaces from both experimental investigations and theoretical calculations [3–7]. For example, oxygen has been shown to strongly activate the oxygen–, carbon–, sulfur–, and nitrogen–hydrogen bonds on transition metal surfaces [8–10], but also to inhibit their dissociation [11–13]. Although it is generally agreed that the formation of strong chemisorbed atomic oxygen poisons active surface sites and is responsible for inhibition, the nature of the activation process remains unclear. To explore the effect of preadsorbed oxygen on the activity of the transition metals, our concern here is to gain more insight from the water dissociation.

Water dissociation is an excellent means for studying some catalysis processes due to its simplicity and importance in such surface reactions as the water–gas shift reaction and Fischer–Tropsch synthesis of hydrocarbons. Thiel and Madey [14] and Henderson [15] have provided comprehensive reviews on the water interaction with clean and oxygen-preadsorbed single-crystal metal surfaces and real catalyst surfaces. From the analysis of Henderson [15], it can be inferred that on one hand preadsorbed oxygen atoms exhibit varying degrees of inducing activity toward water dissociation on many metals [e.g., on Ag(111), Ag(110), Au(110), Cu(111), Cu(100), Pd(111), Pd(110), Rh(100), Rh(111), and Pt(111)], but on the other hand, preadsorbed oxygen atoms either have no influence on or inhibit water dissociation on some surfaces, such as Ru(0001), Ni(111), and Re(001). Even though the effect of preadsorbed oxygen on the water dehydrogenation reaction has been studied

* Corresponding authors. Fax: +86 22 23502458.
E-mail addresses: wangguichang@nankai.edu.cn (G.-C. Wang), buxh@nankai.edu.cn (X.-H. Bu).

0021-9517/$ – see front matter
doi:10.1016/j.jcat.2006.07.034

extensively for decades, the atomic-level mechanisms of this effect remain not well understood. Thus, further investigation is needed to fully understand how water dissociation reactivity is modified by the preadsorbed oxygen on different transition metal surfaces. In this work, we have systematically studied water dissociation on clean and oxygen-preadsorbed Cu(111), Ag(111), Au(111), Ni(111), Rh(111), Pd(111), and Ru(0001) surfaces along with their structures, activation barriers, and total energy changes in detail, by performing self-consistent periodical DFT-GGA calculations.

2. Calculation method and models

To investigate the energy and structural details of water dissociation on clean and oxygen-preadsorbed surfaces, we performed periodic, self-consistent DFT calculation. The GGA with the Perdew, Burke, and Ernzerhof [16] functional was used for the exchange and correlation energy calculation. All calculations were done in simulation tool for atom technology (STATE), which has been successfully applied to study adsorption problems in the case of metal surfaces [17,18]. Ion cores were treated by Troullier–Martines-type norm-conserving pseudopotential [19], and valence wave functions were expanded by a plane wave basis set with a cutoff energy of 25 Ry. The metal surfaces were modeled by a periodical array of three-layered slabs separated by ∼10 Å of vacuum region. A p(3 × 2) unit cell was chosen, which means a monolayer of adsorbates with coverage of 1/6 ML. In calculations, a Monkhorst–Pack mesh of 4 × 6 × 1 special k-point sampling in the surface Brillouin zone was used.

In this work, the adsorption energy (Q_{ads}), or binding energy (BE), of species A on metal surfaces (M) is calculated according to the formula $\mathrm{BE(A)} = E_{\mathrm{A/M}} - E_{\mathrm{M}} - E_{\mathrm{A}}$, where E is the calculated total energy. For a reaction like AB = A + B, the calculated heats of reaction (or total energy change) for those reactions are given by $\Delta H = E_{(\mathrm{A+B})/\mathrm{M}} - E_{\mathrm{AB/M}}$, where $E_{(\mathrm{A+B})/\mathrm{M}}$ is the total energy for the co-adsorption system of A/B/M. The reaction paths of water dissociation on metal surfaces are investigated by the NEB method [20–22]. The transition-state search is initiated by interpolating a series of images of the system between the initial and final states on the potential energy surface. On the potential energy surface, a spring force between the adjacent images is added to keep the spacing between the images constant, and the true force is applied to keep the images sliding toward the minimum-energy path (MEP), thus mimicking an elastic band. Each image is optimized with the NEB algorithm. This approach helps the images converge to the reaction path being searched, and also helps locate the highest point of the MEP. The highest point of the optimized reaction coordinate along the MEP should be the transition state along the chosen reaction path, and this highest energy relative to that of the initial state gives the activation barrier of the reaction. In fact, the modified NEB method (i.e., ANEBA method [23]) is used to increase the density of images near the transition state (TS) and to locate the TS more accurately.

In the ANEBA method, we choose three movable images connecting two local minima on the potential energy surface and use the NEB method as a starting level. After the calculation converges to some given accuracy, we choose the two images adjacent to the one that has the highest energy as our new starting points for the next-level NEB calculation. Through several such levels of NEB calculation, at the last level, the ANEBA calculation will locate three images in which the total energy of each is almost the same; the image in the middle is considered the TS. Although this approach does not use frequency analyses, it has been shown to give excellent convergence to saddle points on the analytical potential energy surface in many cases [24–27].

To test the applicability of the ANEBA method, we compared the results from the conventional NEB and ANEBA methods, taking water dissociation on a clean Cu(111) surface, for example. First, we used the conventional NEB method. We chose a large number of images (16 images) to bracket the saddle point with high accuracy, and obtained a barrier of 1.42 eV. Then we used the ANEBA method, increasing the resolution in the neighborhood of the saddle point; the final saddle point has a maximal force <50 kJ/mol/nm. Four-level recursion of ANEBA was made; the reaction barrier turns out to be nearly the same (1.40 eV). As we can see, the ANEBA is applicable and more efficient than the conventional NEB method.

3. Results and discussion

We determined the most stable initial state (IS) for the H_2O and the $H_2O + O$ co-adsorbed system on each transition metal surface. The ISs (Fig. 1a) are similar; the top site is favored for H_2O on the clean metal surfaces, in agreement with the results of Gao and co-workers [28] and Michaelides et al. [29]. Similarly, the ISs on oxygen-preadsorbed surfaces (Fig. 1b) are alike; O atom is on the fcc site (Cu, Ag, Au, Ni, Pd, Rh) or the hcp site (Ru) [30–32] and H_2O is on the top site, involving one

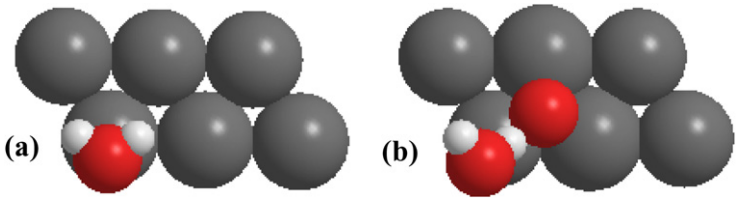

Fig. 1. Top view of the ISs of water dissociation on clean (a) and oxygen preadsorbed (b) metal surfaces. The grey ball represents the metal atom, the white ball represents H, and the red ball represents O.

Table 1
Calculated reaction energies and structure properties of ISs of water dissociation on clean and oxygen preadsorbed metal surfaces

Metal	Clean surface $H_2O = H + OH$			Oxygen preadsorbed surface $H_2O = H + 2OH$		
	E_a (eV)	ΔH (eV)	R_{H-O}[a] (Å)	E_a (eV)	ΔH (eV)	R_{H-O} (Å)
Au	2.24	1.77	0.984	0.61	0.50	1.003
Ag	1.95	0.99	0.985	0.50	−0.16	1.005
Cu	1.40	0.26	0.985	0.76	−0.14	0.999
Pd	1.12	0.01	0.981	0.48	0.38	0.989
Rh	1.08	0.10	0.983	0.71	0.13	0.993
Ni	0.74	−0.56	0.986	0.65	0.29	0.990
Ru	0.90[b]	−0.35	0.993	0.74	0.26	0.990

[a] R_{H-O} is the distance between dissociated H and O involved in water.
[b] The activation energy of the dissociation of a water on clean Ru(0001) is in broad agreement with that of 0.85 eV calculated by Michaelides et al. [30].

Table 2
Coupling matrix element squared, d-bond centre of metals; Q_O, Q_{OH}, and $\Delta\Delta E$

Metal	Au	Ag	Cu	Pd	Rh	Ni	Ru
ε_d (eV)	−3.56	−4.30	−2.67	−1.83	−1.73	−1.29	−1.41
V_{ad}^2 (eV)	3.35	2.26	1.0	2.78	3.32	1.16	3.87
Q_O[a] (eV)	2.66	3.13	4.33	4.44	4.85	5.42	5.62[c]
Q_{OH}[a] (eV)	1.57	2.58	2.82	2.60	2.92	3.18	3.24
$\Delta\Delta E$[b] (eV)	1.63	1.45	0.64	0.64	0.37	0.09	0.16

[a] Q_O and Q_{OH} is the adsorption energy of oxygen and hydroxyl on metal surfaces.
[b] $\Delta\Delta E$ is the difference in the reaction barriers of water dissociation on clean metal surfaces vs on oxygen preadsorbed metal surfaces.
[c] The calculated adsorption energy of oxygen on Ru(0001) is in agreement with the result of Stampfl and Scheffler [31]. (5.55 eV on p(2 × 2) model.)

atom H of H_2O interacting with the preadsorbed O atom. The optimized O–H bond length of the ISs is listed in Table 1. The resulting intermediates of O–H scission in H_2O are H and OH on clean metal surface, and two hydroxyl radicals on oxygen-preadsorbed metal surface. To determine the most stable final state (FS), we investigated the configurations and the energies when OH adsorbed on the top, bridge, and fcc (the hcp on Ru) sites on Cu(111), Ni(111), Pd(111), and Ru(0001) respectively. The results show that the hydroxyl radical adsorbs preferentially on the fcc (hcp on Ru) site with the O–H axis normal to the metal surface. The adsorption energy of OH on metals is given in Table 2. The FSs (Fig. 2a) on clean metal surfaces are similar, and the H and OH on clean surface are placed above the two closest fcc (hcp on Ru) sites. The FSs (Fig. 2b) on oxygen-preadsorbed surfaces are also similar, with the two hydroxyls adsorbed on two closest fcc (hcp on Ru) sites.

Following the NEB method, structural changes of intermediates for these reactions can be approximated by interpolating a series of images between the reactants and the products under a full optimization of the coordinates of these adsorbed species. Calculated snapshots of structural changes of intermediates in water dissociation on clean and oxygen-preadsorbed Ag(111) are given in Fig. 3. The TS structure properties thus obtained are given in Table 3 and shown in Fig. 4. Directly comparing the structure of TS, reactant, and product shows that on the clean surfaces, the TSs are all the "final state-like"; on oxygen-preadsorbed surfaces, the TSs are also "final state-like" on Pd and Ni, whereas the TSs on Au, Ag, Cu, Rh, and Ru are "initial state-like." The reaction barriers (E_a) and total energy change (ΔH) are also given in Table 1. It shows clearly that the reaction barrier on each oxygen-preadsorbed surface is lower than that on clean surfaces. The calculated results are in broad agreement with experimental observations reported in the review of Henderson [15].

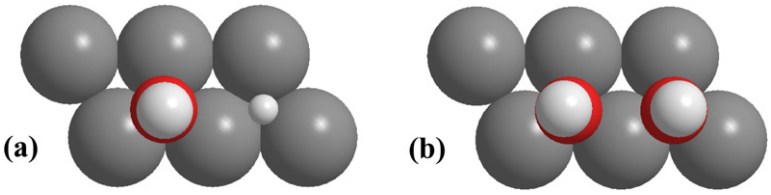

Fig. 2. Top view of the FSs of water dissociation on clean (a) and oxygen preadsorbed (b) metal surfaces. The grey ball represents the metal atom, the white ball represents H, and the red ball represents O.

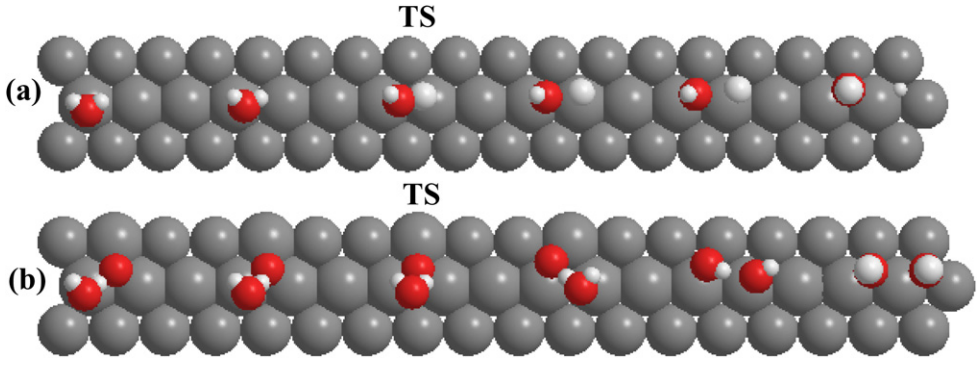

Fig. 3. Calculated snapshot of structural changes of intermediates in water dissociation on clean (a) and oxygen preadsorbed (b) Ag(111). The grey ball represents the Ag atom, the white ball represents H, and the red ball represents O.

Table 3
Properties of the TSs of water dissociation on clean and oxygen preadsorbed metal surfaces

Metal	Clean surface					Oxygen preadsorbed surface				
	$R_{OM(\perp)}$[a]	$R_{(HO)}$	$R_{HM(\perp)}$	R_{HM}	TS type[b]	$R_{H_2OM(\perp)}$	$R_{OM(\perp)}$	$R_{(HO)}$	∠(HOH)	TS type
Au	1.822	2.065	1.414	1.597	Final	3.142	1.452	1.001	97.3	Initial
Ag	1.905	1.789	1.544	1.687	Final	3.268	1.264	0.983	97.5	Initial
Cu	1.713	1.670	1.416	1.562	Final	3.268	1.293	0.994	97.0	Initial
Pd	1.819	1.543	1.481	1.543	Final	2.369	1.517	2.415	Dissociated	Final
Rh	2.002	1.543	1.534	1.666	Final	3.058	1.387	0.991	99.5	Initial
Ni	1.651	1.881	1.291	1.543	Final	2.748	1.357	1.465	Dissociated	Final
Ru	2.010	1.426	1.818	1.688	Final	2.963	1.338	0.991	99.5	Initial

[a] All distances in angstroms, angles in degrees.
[b] The "initial" represents the transition state is "initial-state-like," and the "final" represents the transition state is "final-state-like."

3.1. Water dissociation on clean metal surfaces

The development of general structure–property relationships relating the activity of metal surface to its fundamental electronic and structural properties has been a long-standing goal in heterogeneous catalysis [33]. In the present work, we first analyzed water dissociation on clean metal surfaces. To understand the relationship between the changes in reaction energy and the electronic properties of the surface, we analyzed the surface properties on the basis of the method proposed by Hammer and Nørskov [34], that the BEs and dissociation energies of adsorbates correlate linearly with the d-band center for various metals, and that this correlation exists only for the same type of binding mode. Fig. 4a shows that our results are consistent with the theoretical model; that is, the closer of d-band center to the Fermi level, the lower the reaction barrier. All of the four metals shown in Fig. 5a are group VIII metals, which have unfilled (but more than half-filled) d shells. For copper, silver, and gold, each of which has a filled d band, a different parameter—the adsorbate states-metal d-band coupling matrix element V_{ad}^2 [34]—can linearly correlate with the reaction barriers (Fig. 5b). The relationship suggests that the stronger the overlap (i.e., the larger the repulsion), the higher the reaction barrier. As we can see, the d-bond center decreases from the left to the right of the periodic table in the transition series and is complete at the noble metals Cu, Ag, and Au; however, the size of the coupling matrix element always increases down through each of the groups of the periodic table, making the 5d metals the most noble ones, and thus the dissociation energy becomes larger and larger from Cu to Au. As analyzed above,a periodic trend for the chemical activity of various transition metals for water dissociation can be determined: Chemical activity increases from right to left of the periodic table and decreases down through each group on the periodic table.

Another classical approach to developing quantitative activity correlations with predictive utility in homogeneous catalysis is the formation of Brønsted–Evans–Polanyi (BEP) relationship. In principle, the development of BEP relationship for surface reactions could provide the means for correlating and predict variations in activity and selectivity between metals [35–37]. For water dissociation on clean surfaces, a detailed analysis was carried out based on thermodynamic effects, and a good linear correlation was found between the reaction barriers and the total energy changes, as shown in Fig. 6. The BEP relationship that we identify for water dissociation (in eV) is $E_a = (0.67 \pm 0.05)\Delta H + (1.13 \pm 0.04)$, in agreement with the result estimated by Pallassana and Meurock [38]. In their work, a slope of 0.65 was obtained for reactions in which bonds containing hydrogen were broken. Michaelides et al. [39] also identified a fundamental BEP relationship for dehydrogenation reactions (in eV), $E_a = (0.92 \pm 0.05)\Delta H + (0.87 \pm 0.05)$. Note that this class includes many kinds of dehydrogenation reactions, including O–H cleavage in H_2O, OH, and CH_3OH; N–H cleavage in NH_3 and NH_2; S–H cleavage in H_2S; and SH or C–H cleavage in CH_x fragments on different metals. There may be different reaction mechanics for different species, so the system is somewhat different with water dissociation on metals with similar mechanics and TSs. It can be seen that the more negative the total energy change, the smaller the barrier. Therefore, the more negative the total energy change of H_2O decomposition (i.e., the products are more stable than reactants), the more active the corresponding metal. The result of chemical activity of metals is in good agreement with the analysis from the electronic factor above. The reason for the BEP relationship is clearly that the transition states (TSs) involve the same bond and their geometrical properties are the same—"final state-like" for all of the metals.

3.2. Water dissociation on oxygen-preadsorbed metal surfaces

For water dissociation on oxygen-preadsorbed metal surfaces, the hydrogen abstraction mechanism by the preadsorbed oxygen atom is significantly different than the mechanism by which water is activated on clean metal surfaces—through hydrogen abstracted from water by oxygen to produce hydroxyl ($H_2O + O = 2OH$) [15]. In the path of water dissociation on oxygen-preadsorbed metal surface, water is assumed, under the attractive interaction between the H of H_2O and the preadsorbed O atom, to move to the adsorption site of O first, after which the OH bond-breaking in H_2O and the OH bond-forming with the O_{ads} occur simultaneously in the TS. In fact, in the reaction process, hydrogen abstraction from water molecules on the metal surface occurs together with a translation of the product species toward their preferred adsorption sites. This process is illustrated in Fig. 3b, which provides a snapshot of structural changes of intermediates in water dissociation on oxygen-preadsorbed Ag(111). It can be seen from Table 1 that for water

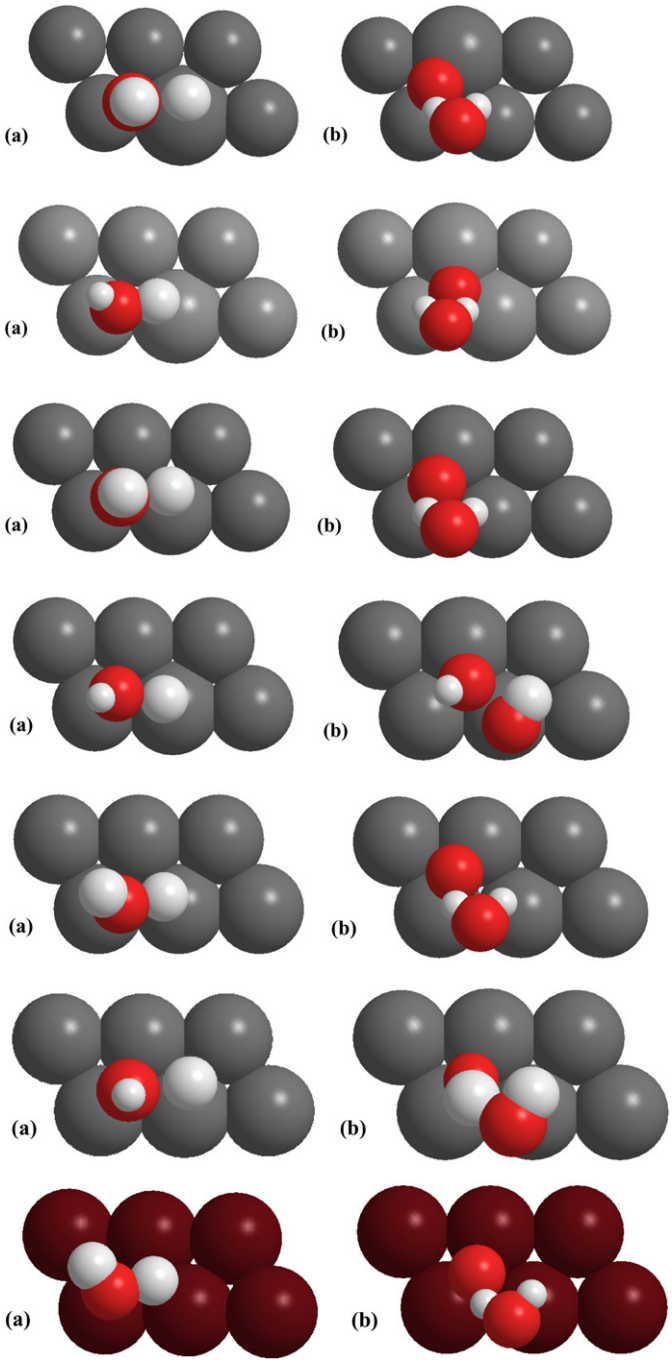

Fig. 4. Top view of the TSs of water dissociation on clean (a) and oxygen preadsorbed (b) metal surfaces. They are presented in the follow order: Au(111), Ag(111), Cu(111), Pd(111), Rh(111), Ni(111), and Ru(0001). The grey ball represents the metal atom except Ru, and the scarlet ball represents the Ru atom. The white ball represents H, and the red ball represents O.

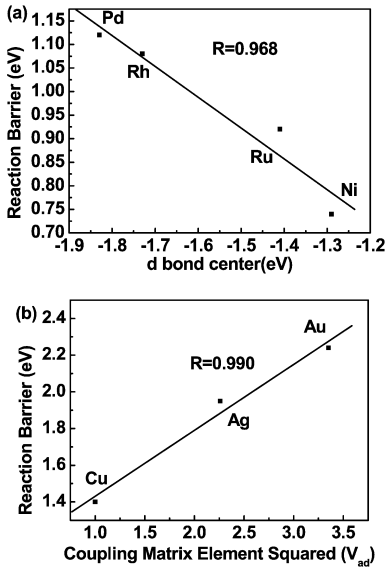

Fig. 5. (a) Plot of the calculated reaction barrier for water dissociation on Pd, Rh, Ni, and Ru versus the d-band center (ε_d); (b) on Cu, Ag, and Au against the coupling matrix element squared (V_{ad}^2). R is the correlation coefficient.

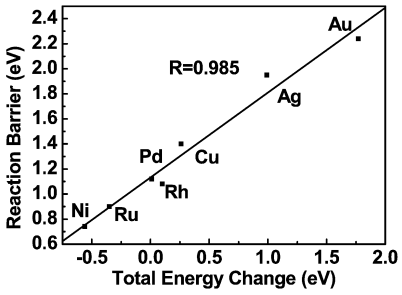

Fig. 6. Relationship of reaction barrier for water dissociation on clean metals and the total energy change, R is the correlation coefficient.

dissociation, the presence of preadsorbed oxygen atoms dramatically decreases the value of barriers on Au(111), Ag(111) and Cu(111) and moderately decreases the barriers on Pd(111) and Rh(111), and also that preadsorbed oxygen has little effect on the reaction barriers on Ni(111) and Ru(0001). Moreover, the calculated barriers for water dissociation on oxygen-preadsorbed metals cannot be well correlated with the d-bond center; the BEP relationship fails in such cases. A possible reason for the failure of the BEP relationship may be that the TS type for the water dissociation may be different on the oxygen-preadsorbed metal surfaces. For example, if the atomic oxygen strongly binds to the transition metal, then a weak interaction will form between the adsorbed oxygen atoms and the breaking hydrogen atoms involved in water molecules. That is to say, the preadsorbed oxygen has a little effect on the water dissociation mechanism, and the properties of TSs may be the same on the oxygen atom-modified metal surface as on the clean surface. On the other hand, if the oxygen atoms have a weakly interaction with the metal, then a strong interaction will form between the adsorbed oxygen atoms and the breaking hydrogen atoms involved in water molecules, so the reaction mechanism will be intensively affected by the preadsorbed oxygen atoms, and the transition state properties will be changed. Therefore, the TS type of water dissociation on preadsorbed transition metals is not the same for all metals; it depends on the nature of transition metals. Indeed, checking the structure of TS, we find that the TSs of Au, Ag, Cu, Rh, and Ru changed from the original "final state-like" (i.e., in the case of water dissociation on clean metal) to "initial state-like" (Fig. 4) in the presence of oxygen;

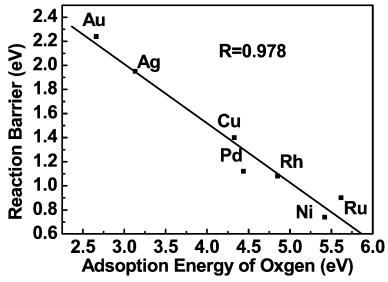

Fig. 7. Relationship of reaction barrier for water dissociation on clean metals and the adsorption energy of atomic oxygen, R is the correlation coefficient.

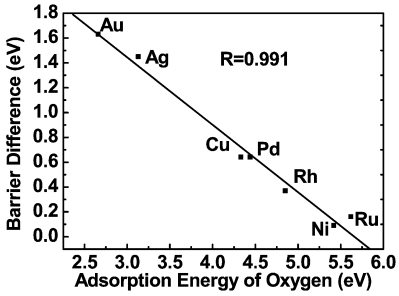

Fig. 8. Relationship of reaction barrier difference for water dissociation on clean and oxygen preadsorbed metal surface and the adsorption energy of atomic oxygen, R is the correlation coefficient.

in contrast, the TSs on Pd and Ni metals remain "final state-like."

3.3. Relationship between adsorption energy of oxygen and the promoted effect

Interestingly, comparing the breaking O–H bond length on oxygen-preadsorbed surfaces with that on clean metal surfaces demonstrates that the bond length on oxygen-preadsorbed surfaces becomes greater than that on clean surfaces except on Ru(0001) (Table 1), which is consistent with the reaction barrier results demonstrating that the water readily dissociates on oxygen-preadsorbed metal surfaces. Now the question arises as to why can the preadsorbed oxygen affects the activity of the metals. To answer this question, we calculated the adsorption energies of oxygen atoms on the metal surfaces (Table 2) and found interesting results (Figs. 7 and 8). Fig. 7 shows that the adsorption energy of oxygen is in consistent with the chemical activity of metals on clean surfaces (i.e., the greater the adsorption energy, the more active the metal). Fig. 8 shows a nice linear relationship between adsorption energies of oxygen atom and the difference in the reaction barrier of water dissociation on a clean surface versus that on an oxygen-preadsorbed surface (i.e., the smaller the value of the atom oxygen adsorption energy, the larger the barrier difference and the greater the promoted effect). Carefully examining Figs. 7 and 8, we can write the BEP relationships (in eV) as

$$E_{a1} = a_1 E_O + b_1, \tag{1}$$

where E_{a1} is the reaction barrier of water dissociation on clean metals, E_O is the adsorption of O atom, and a_1 and b_1 are coefficients from Fig. 7. The reaction barrier difference is $dE = E_{a1} - E_{a2}$, where E_{a2} is the reaction barrier on oxygen-preadsorbed surface. According to Fig. 8,

$$dE = a_2 E_O + b_2, \tag{2}$$

where a_2 and b_2 are coefficients.

Closely examining the data in Figs. 7 and 8, we find that

$$E_{a1} = -(0.49 \pm 0.04) E_O + (3.48 \pm 0.20)$$

and

$$dE = -(0.54 \pm 0.03) E_O + (3.07 \pm 0.14).$$

It appears that the regression coefficients a_1 and a_2 are very close in value, and thus the difference $(a_1 - a_2)$ approaches zero. This finding suggests that the reaction barrier for hydrogen abstraction on oxygen-preadsorbed surfaces is approximately constant—that is, it does not depend on the surface, which is consistent with the data given in Table 1 (the barriers are all in the range 0.48–0.76 eV). Thus, preadsorbed oxygen makes different metals have similar activity for water dissociation, but it has different inducing effect on different metals. This different inducing effect, can be explained by the fact that the preadsorbed oxygen can interact with both the metal atoms and the breaking hydrogen atoms from H_2O molecules. There is competition between the formation of the metal–oxygen bond (O–M) and the formation of the hydrogen–oxygen bond (O–H). Obviously, *the more strongly bound the oxygen atoms on the metal surface, the less promoted the effect of water on O–H bond scission*. The varying H–O bond lengths given in Table 1 provide evidence of this effect. The promoted effect of preadsorbed oxygen (at coverage of 1/6 ML) decreases in the order Au > Ag > Cu > Pd > Rh > Ru > Ni and is projected to be reversed in the order Au < Ag < Cu < Pd < Rh < Ru < Ni on clean surfaces.

4. Conclusion

The present work provides a systematical theoretical study of water dissociation on clean and oxygen-preadsorbed transition metals. We report periodic trends for water dissociation on both clean and oxygen-preadsorbed surfaces. For clean surfaces, the chemical activity increases in the order Au < Ag < Cu < Pd < Rh < Ru < Ni. However, the inducing effect of preadsorbed oxygen decreases in the above order from facilitating O–H bond cleavage on the least active metals, such as Au (or Ag), to having little or no effect on this process on the active metals, such as Ni and Ru. These findings suggest that preadsorbed oxygen plays an important role in industrial reactions on transition metal catalysts. Furthermore, using oxygen and other preadsorbed impurities to systematically alter or fine-tune the catalytic properties of transition metal surfaces can be envisioned.

Acknowledgments

G.C. Wang thanks Dr. Junji Nakamura of Tsukuba University for valuable discussions. This work was supported

by the National Natural Science Foundation of China (grant 20273034) and the NKStar HPC program, as well as the Large-Scale Numerical Simulation Project of Science Information Center of University of Tsukuba, Japan.

References

[1] G. Ertl, H. Knözinger, J. Weitkamp (Eds.), Handbook of Heterogeneous Catalysis, VCH, Weinheim, 1997.
[2] R.I. Masel, Principles of Adsorption and Reaction on Solid Surface, Wiley, New York, 1996.
[3] M. Neurock, A. van Santen, W. Biemolt, A.P.J. Jansen, J. Am. Chem. Soc. 116 (1994) 6860.
[4] S. Yamagishi, S.J. Jenkins, D.A. King, J. Am. Chem. Soc. 126 (2004) 10962.
[5] I.E. Wachs, R.J. Madix, J. Catal. 53 (1978) 208.
[6] R.B. Barros, A.R. Garcia, L.M. Ilharco, J. Phys. Chem. B 108 (2004) 4831.
[7] S. Sakong, A. Grob, J. Catal. 231 (2005) 420.
[8] E. Shustorovich, A.T. Bell, Surf. Sci. 268 (1992) 397.
[9] C.T. Au, M.W. Roberts, Chem. Phys. Lett. 74 (1980) 472.
[10] B.A. Sexton, A.E. Hughes, N.R. Avery, Surf. Sci. 155 (1985) 366.
[11] B. Afsin, P.R. Davies, A. Pashuski, M.W. Roberts, Surf. Sci. Lett. 259 (1991) 724.
[12] B. Afsin, P.R. Davies, A. Pashusky, M.W. Roberts, D. Vincent, Surf. Sci. 284 (1993) 109.
[13] A. Boronin, A. Pashusky, M.W. Roberts, Catal. Lett. 16 (1992) 345.
[14] P.A. Thiel, T.E. Madey, Surf. Sci. Rep. 7 (1987) 211.
[15] M.A. Henderson, Surf. Sci. Rep. 46 (2002) 1–308.
[16] J.P. Perdew, K. Burke, M. Ernzerhof, Phys. Rev. Lett. 77 (1996) 3865.
[17] G.C. Wang, Y. Morikawa, T. Matsumoto, J. Nakamura, J. Phys. Chem. B 110 (2006) 9.
[18] S. Smsuda, R. Szuki, M. Aoki, Y. Morikawa, R. Kishi, K. Kawai, J. Chem. Phys. 114 (2001) 8546.
[19] G. Schenter, G. Mills, H. Jónsson, J. Chem. Phys. 101 (1994) 8964.
[20] G. Mills, H. Jónsson, G. Schenter, Surf. Sci. 324 (1995) 305.
[21] G. Henkelman, H. Jónsson, J. Chem. Phys. 113 (2000) 9978.
[22] G. Henkelman, B.P. Uberuaga, H. Jónsson, J. Chem. Phys. 113 (2000) 9901.
[23] P. Maragakis, S.A. Andreev, K. Brumer, D.R. Reichman, E. Kaxiras, J. Chem. Phys. 117 (2002) 4651.
[24] K.D. Sanket, N. Matthew, K. Kourtakis, J. Phys. Chem. B 106 (2002) 2559.
[25] J. Greeley, M. Mavrikakis, J. Catal. 208 (2002) 291.
[26] J. Greeley, M. Mavrikakis, J. Am. Chem. Soc. 124 (2002) 7193.
[27] G.C. Wang, Y.H. Zhou, Y. Morikawa, J. Nakamura, Z.S. Cai, X.Z. Zhao, J. Phys. Chem. B 109 (2005) 65.
[28] S. Meng, E.G. Wang, S. Gao, Phys. Rev. B 69 (2004) 195404.
[29] A. Michaelides, V.A. Ranea, P.L. de Andres, D.A. King, Phys. Rev. Lett. 90 (2003) 216102.
[30] A. Michaelides, A. Alavi, D.A. King, J. Am. Chem. Soc. 125 (2003) 2746.
[31] C. Stampfl, M. Scheffler, Phys. Rev. B 54 (1996) 2868.
[32] C. Stampfl, S. Schwegmann, H. Over, M. Scheffler, G. Ertl, Phys. Rev. Lett. 77 (1996) 3371.
[33] R.A. Van Santen, Theoretical Heterogeneous Catalysis, World Scientific, Singapore, 1991.
[34] B. Hammer, J.K. Nørskov, Adv. Catal. 45 (2000) 71.
[35] M. Mavrikakis, M.A. Barteau, J. Mol. Catal. A Chem. 131 (1998) 135.
[36] A.J. Gellman, Q. Dai, J. Am. Chem. Soc. 115 (1993) 714.
[37] S. Dahl, A. Logadottir, C.J.H. Jacobsen, J.K. Nørskov, Appl. Catal. A 222 (2001) 19.
[38] V. Pallassana, M. Meurock, J. Catal. 191 (2000) 301.
[39] A. Michaelides, Z.P. Liu, C.J. Zhang, A. Alavi, D.A. King, P. Hu, J. Am. Chem. Soc. 125 (2003) 3704.